Results in Engineering 25 (2025) 103679

Contents lists available at ScienceDirect

Results in Engineering

journal homepage: www.sciencedirect.com/journal/results-in-engineering

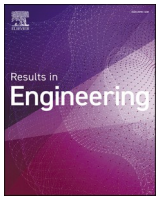

Research paper

Biomass pyrolysis for biochar production: Study of kinetics parameters and effect of temperature on biochar yield and its physicochemical properties

Nikhill Rambhatla [a], Tanushka Florence Panicker [a], Ranjeet Kumar Mishra [a,*], Srinivas Kini Manjeshwar [a,*], Abhishek Sharma [b]

[a] Department of Chemical Engineering, Manipal Institute of Technology, Manipal Academy of Higher Education, Manipal, Karnataka-576104, India
[b] Department of Biotechnology & Chemical Engineering, Manipal University Jaipur, Rajasthan 303007, India

ARTICLE INFO

Keywords:
Waste sawdust
Pyrolysis
Kinetics study
Biochar
Activation energy
Surface morphology

ABSTRACT

This study investigates the pyrolysis kinetics behaviour and temperature effects on biochar yield and properties during pyrolysis. The kinetic study of biomass was performed using a thermogravimetric analyser at dynamic heating rates (10, 30, and 50 °C min^{-1}) in an inert atmosphere. The kinetic parameters were estimated using Kissinger-Akahira-Sunose (KAS), Distributed Activation Energy Model (DAEM), and Vyazovkin model (VZ). The pyrolysis experiment was performed in a stainless steel semi-batch reactor at 400, 600, and 900 °C, 10 °C min^{-1} heating rate, 45 min holding time and 100 mL min^{-1} nitrogen gas flow rate. The produced biochar was characterised using proximate analysis, ultimate analysis, heating value, bulk density, BET surface area analyser, TGA, FTIR, and FE-SEM analysis. The physicochemical results support the candidacy of biomass for biochar and fuel production. Further, the kinetic analysis of MWS using KAS, DAEM, and VZ was found to be 233.39, 238.11, and 224.74 kJ mol^{-1}, respectively. The experimental results reveal that higher temperatures (600 and 900 °C) generally reduce biochar yield (19 %) due to increased devolatilization but enhance the biochar's surface area (17 %) and carbon content (4.84 %). The characterisation results of biochar confirmed higher carbon content (76.02 wt. %), HHV (36.97 MJ kg^{-1}), and significant oxygen content (22.01 %) at 900 °C. Also, the thermal profile and surface morphology of the biochar suggest that biochar derived at 600 and 900 °C can be used for carbon-based applications, whereas biochar derived at 400 °C can be used for soil amendment or fertiliser applications.

1. Introduction

Fossil energy sources, including coal, natural gas, and petroleum, currently provide around 80 % of the world's energy demands. Despite being the world's primary energy source, fossil fuels have finite supplies and can cause huge environmental issues, including air pollution and global warming [1,2]. About 30 % of the world's energy demands are currently met by coal, and if current usage trends continue, there is an estimated 118 years' worth of coal in the world's reserves [3]. By 2030, the carbon emission footprint is predicted to quadruple from its 2004 level due to the increased use of coal [3]. The drawbacks of utilising fossil fuels have led to a daily increase in studies on renewable energy sources, including biomass, solar, wind, and hydraulics [4,5]. Although it can be processed into a variety of biofuels, including biogas, bioethanol, biodiesel, and charcoal, biomass is regarded as a significant renewable energy source. Researching renewable energy sources is one of humanity's most enormous difficulties because of the need to find sources that can meet the consumption of energy and the reliance on fossil fuels for energy. Renewable energy sources, like biomasses, offer various benefits, including being renewable and not contributing to global warming [6]. From a long-term viewpoint, biomass seems to play an essential part in energy, environmental, and socioeconomic aspects [7]. The hunt for renewable energy sources has advanced over the past few years, which has helped to lower the need for fossil fuels [8].

Understanding and optimising the thermal breakdown method to produce the desired products requires an understanding of the thermodynamic and kinetic factors that influence the thermos conversion processes of biomass. Research on pyrolysis kinetics is essential for assessing the viability, scalability, and design of biomass conversion reactors in industrial settings [9]. The yield and composition of each phase produced vary depending on the reaction parameters and biomass components [10]. Along with other key influencing factors, the process

E-mail addresses: ranjeet.mishra@manipal.edu (R.K. Mishra), srinivas.kini@manipal.edu (S.K. Manjeshwar).
* Corresponding author.

https://doi.org/10.1016/j.rineng.2024.103679
Received 11 November 2024; Received in revised form 2 December 2024; Accepted 7 December 2024
Available online 7 December 2024

products depend on the reactor for the duration of the biomass's maintenance at a specific temperature. Finally, understanding these factors is necessary for the construction of a reactor that uses the pyrolysis process [11]. The reactor type and the mathematical modeling used are additional aspects that affect the estimation of kinetic parameters, in addition to variables like temperature, heating rate, residence time, and atmosphere type [11]. In the research and development stage, a mathematical model is applied to ascertain feasible processes and kinetic variables from the reaction data in the lab and in the pilot plant [12]. The data required to establish these parameters is obtained through the investigation of the effects of various operating environments for optimization studies. The activation energy (E_a), frequency factor, and order of reaction (n) are the key variables for kinetic analysis. Distributed Activation Energy Model (DAEM) assumes a distribution of activation energies to describe the complex kinetics of biomass pyrolysis. Vyazovkin model (VZ) uses isoconversional methods to determine the activation energy without assuming a specific reaction model. The Kissinger-Akahira-Sunose (KAS) method estimates activation energy based on the temperature at different heating rates. These models help in understanding the thermal decomposition behaviour of biomass during pyrolysis [12]. Distributed Activation Energy Model (DAEM) assumes a distribution of activation energies, capturing the complexity of biomass pyrolysis. Vyazovkin model (VZ) calculates activation energy across conversion rates without assuming a reaction model, offering flexibility. The Kissinger-Akahira-Sunose (KAS) method also estimates activation energy but relies on temperature changes at different heating rates, making it more straightforward but less detailed than DAEM [12]. Numerous approaches have been devised to determine the kinetic parameters of the reactions, which are based on the Arrhenius equation [13]. Most studies employ thermal data for the thermal breakdown reaction of biomass; however, there still needs to be more research in the literature about the use of factorial planning with chemical process data to determine the kinetic parameters of biomass. The advancement of research depends on experimental design, a mathematical strategy that methodically links the variables and yields the needed results in the shortest period.

Biofuels and biochar can be produced from biomass using a variety of processes, which are split into two primary categories: biological (BCP), and thermochemical (TCP) [13]. Thermochemical methods are acknowledged as essential pathways for converting biomass into chemicals and fuels [14]. Pyrolysis is one of the thermochemical processes that turn biomass into biofuels. It is done in a non-oxidizing atmosphere at relatively moderate temperatures (400–800 °C) [15]. The process leaves behind a solid residue rich in carbon (coal), a volatile phase made up of gases and condensable organic vapours [16]. Numerous chemical groups and classes of chemicals are found in the composition of the pyrolytic liquid [17,18]. Pyrolysis can be classified into three main categories based on the residence time: (i) slow pyrolysis, (ii) fast pyrolysis, and (iii) flash pyrolysis [19]. Slow pyrolysis is a significant industrial process that predominantly yields char and is employed for producing solid fuel [9,20]. Alternatively, the most promising path to produce sustainable chemicals and fuels has been identified as fast pyrolysis.

Biochar is a carbon-rich material produced by heating biomass under oxygen-limited conditions (pyrolysis). It is widely used to improve soil fertility, enhance water retention, and sequester carbon, aiding in climate change mitigation. Additionally, biochar serves in waste management, pollutant adsorption, and as a precursor for advanced functional materials [21]. Many studies have been carried out to produce biochar from biomass. Manyà et al. (2018) produced biochar through slow pyrolysis of different biomass materials in a fixed-bed pyrolysis reactor [22]. The results of the statistical studies showed that the peak temperature and, to a lesser degree, the biomass had the most incredible effects on the attributes of biochar related to its potential stability. When the pressure was increased, a noticeable rise in the generated gas yield was detected. Selvarajoo and Oochit (2020) produced the biochar from the pyrolysis of palm fibre from 300–900 °C at a heating rate of 5 °C min^{-1} [3]. They reported that maximum char yield was obtained at lower temperatures, whereas improved characteristics of biochar were found at higher temperatures [3]. Sahoo et al. (2021) produced the biochar from pigeon pea stalks and bamboo biomass at 400, 500, and 600 °C for a holding time of 1 h [23]. They reported that biochar produced at lower temperatures has a lower heating value (LHV) and maximum biochar yield; however, at higher temperatures, yield is reduced, and properties of biochar are increased [23]. De Almeida et al. (2022) produced the biochar from sugarcane biomass at 450, 550, and 650 °C and 10 °C min^{-1} in a bench-scale fixed-bed reactor [24]. They reported that biochar produced at 450 °C has a greater heating value, higher carbon content, and maximum biochar yield. Suresh Babu et al. (2024) produced the biochar from mixed wood waste (MWS) using slow pyrolysis at dynamic temperatures (400, 600, and 800 oC) and holding times (30, 45, and 60 min) [25]. They reported that by increasing the temperature from 400 to 800 °C, the yield of reduced biochar was reduced while enhancing its carbon content. Higher pyrolysis temperatures (400–800 °C) led to increased HHV and bulk density. Furthermore, BET surface area and zeta potential showed significant improvement across this temperature range. FE-SEM analysis demonstrated that elevated temperatures intensified volatilization, resulting in substantial surface modifications [25].

A literature review highlights the lack of studies on biochar production from mixed wood sawdust and a need for a deeper exploration of temperature effects on its properties. While kinetic studies on biomass are abundant, to the best of the authors' knowledge, the kinetic analysis of mixed wood sawdust using Kissinger-Akahira-Sunose (KAS), Distributed Activation Energy Model (DAEM), and Vyazovkin Model (VZ) method at dynamic heating rates remains unexplored. This study addresses these gaps by analysing the kinetic parameters and examining the influence of temperature on biochar yield and properties during pyrolysis. The kinetic study was performed using KAS, DAEM, and VZ models in a thermogravimetric analyser (TGA) at dynamic heating rates (10, 30, and 50 °C min^{-1}). Furthermore, the pyrolysis experiment was performed in a semo-batch reactor with the inert gas facility at 400, 600, and 900 °C, respectively. The produced biochar was characterised by its physical and chemical properties.

2. Materials and methods

2.1. Sample collection and preparations

Mixed wood sawdust (MWS) was collected from the local wood mill near the Manipal Institute of Technology campus, Udupi district, India. The collected sawdust was sundried over a week and placed in a digital hot air oven (PSI 030) at 105 °C for 3 h for uniform removal of moisture. Further, the dried sawdust was ground in a lab cum mixture grinder to obtain uniform particle size (750 μm) of biomass and stored in an air-tight plastic bag for further experiments.

2.2. Physicochemical characterization of biomass and biochar

All feedstocks are characterised chemically and physically before their prospective applicability is evaluated. The amount of material that burns as volatile matter (gaseous state), fixed carbon (solid-state), and inorganic residue (ash content) is provided by the proximate analysis of feedstock or fuel. Assessments of the volatile matter, ash content, and fixed carbon were made using the ASTM-D 5142 and D1762–84 methods. In addition, ASTM D5373 was employed to estimate C, H, N, and Sulfur using an elemental analyzer (FLASH 2000, Thermo Fisher Scientific Inc., USA), and the difference was used to calculate oxygen. The biochemical components of biomass, such as hemicellulose, cellulose, and lignin, were identified by the wet chemistry method. The biomass bulk density was measured with a digital balance and a measuring cylinder. In contrast, the biomass higher heating value (HHV)

was estimated using an oxygen bomb calorimeter (1341 Plain Jacket Calorimeter, Paar Instrument). The pH of the biochar was determined using an automated titration system (pH meter, Mettler Toledo, USA). Prior to deciding the biochar's pH, the pH meter was calibrated using buffer solutions of 4, 7, and 10. In 50 mL of distilled water, 1 g of moisture-free biochar was dissolved to determine the pH of the material. Once the biochar had been evenly mixed with the distilled water, the mixture was left to stir overnight at 25 °C.

2.3. Thermal stability analysis

The thermal stability of biomass and biochar was examined using a thermogravimetric analyzer (NETZSCH, TG 209 F1 Libra) under oxygen-depleted circumstances. Samples weighing 9±0.05 mg were heated at a rate of 10 °C min^{-1} from 30 to 700 °C while an inert gas flow of 50 mL min^{-1} was continuously maintained. Data from the TGA was retrieved and used in this investigation using universal software. Further, the kinetic study of carryout in the same TGA at multiple heating rates (10, 30, and 50 °C min^{-1}).

2.4. FTIR study

FTIR-ATR (Model No.: IRAffinity-1) was used to evaluate the feedstock's functional groups. On the ATR crystal surface, a small amount of oven-dried sample was applied, and scanning was carried out at a rate of 64 scans per second with a resolution of 4 cm^{-1} over the 400–4000 cm^{-1} wavenumber range.

2.5. XRD analysis of biomass and biochar

A Rigaku TT Rax diffractometer coupled with a Cu-Kα radiation source and an X-ray produced at 15 kW and 250 mA were used to get the XRD pattern of biomass samples. All biomasses were scanned at a scanning angle of 2θ of 10–60° at a speed of 0.03 min^{-1}. The crystallinity index of biomass samples was determined using the formula below.

$$Crl\ (\%) = \left[\frac{I_{crystalline} - I_{amorphoues}}{I_{amorphoues}}\right] \times 100 \quad (1)$$

where the crystalline portion of the biomass sample (cellulose) had a crystalline peak intensity of around 2θ = 22.25, while the amorphous portion (cellulose, hemicellulose, and lignin) had an amorphous peak intensity of 2θ = 16.12.

2.6. Kinetic theory

Different origins result in different compositions for biomass. A precise prediction of the reaction mechanism is practically impossible during pyrolysis due to the fast occurrence of many reactions. Nevertheless, the following simple and all-inclusive biomass degradation reaction is recommended:

$$Biomass\ (solid) \xrightarrow{k(t)} volatile\ (gases + tar) + Char\ (solid\ residue) \quad (2)$$

The Arrhenius temperature expression can be integrated with the conversion function to produce the following equation:

$$g(\kappa) = \int_0^x \frac{dx}{f(x)} = \int_0^T \frac{A}{\delta} e^{-(E/RT)}\, dT \quad (3)$$

$$g(\kappa) = \frac{AE}{\delta R}\int_0^x u^{-2} e^{-u} du = \frac{AE}{\delta R} p(x) \quad (4)$$

where $g(\kappa)$ signifies integral conversion and $x = \frac{E}{RT}$. The value of $p(x)$ is subjected to the forms of approximation. The value of $p(x)$ is subjected to the forms of approximation [26]. The kinetic constraints of the MWS were determined in this study using three model-free techniques: Kissinger-Akahira-Sunose (KAS), Distributed Activation Energy Model (DAEM), and Vyazovkin model (VZ). Past research on kinetics has provided information about the kinetic mathematical origin [27,28]. Equations 5, 6, 7 and 8 were used to determine the kinetics parameters and listed in Table 1. where *n, T, β, R, A,* and *E* are denoted as the reaction order, absolute temperature (K), heating rate (°C min^{-1}), Gas constant ($J\ mol^{-1}.\ K^{-1}$), pre-exponential factor (min^{-1}), and activation energy (KJ mol^{-1}), respectively.

2.7. Experimental setup

MWS pyrolysis experiment was carried out in a semi-batch fixed bed vertical tube pyrolyzer with dimensions (6 cm x 5.4 cm x 34 cm). The pyrolyzer was constructed using ceramic bricks to prevent heat loss, while the exterior is composed of stainless steel (SS-304). Stainless steel in the shape of a cylinder makes up the pyrolysis reactor. The nitrogen cylinder, ceramic stoppers, rector, thermocouple, control panel, and conical flask with a water and gas rotameter are all parts of the pyrolysis setup. While the temperature and heating rates were managed via the control panel, a thermocouple that was attached directly to the reactor continuously monitored the temperature inside the reactor. The tube reactor was filled with the necessary 150 g of sample. Throughout the experiment, the nitrogen gas flow rate was kept constant (1.5 standard liters per minute). The conditions for the pyrolysis trial were carried out at 400, 600, and 900 °C, respectively, with 45 min holding time and 10 °C min^{-1} heating rate. Holding time in pyrolysis refers to the duration for which the material is maintained at the desired pyrolysis temperature. This time is crucial for ensuring the complete thermal decomposition of the material. Furthermore, the reactor was left to cool to ambient temperature (25–30 °C) once the test was completed. The biochar was then collected and kept in an airtight glass jar. The exact biochar yield was confirmed by repeating each pyrolysis test thrice. Finally, Equation 9 was used to calculate the biochar yield. Fig. 1 shows a schematic drawing of the experimental setup for pyrolysis.

$$\%\ Yield\ of\ biocarbon = \left[\frac{Solid\ material\ left\ after\ the\ pyrolysis}{Weight\ of\ feeded\ biooil}\right] \times 100 \quad (9)$$

2.8. Physicochemical characterization of biochar

The proximate analysis, elemental analysis, heating value (HHV), pH, and bulk density analysis were performed using methods mentioned in Section 2.2. A Brunauer-Emmett-Teller (BET) surface area analyzer (Autosorb-iQ, Quantachrome Instruments) with ASiQwin 5 software was used to analyze the BET surface area. To remove pore moisture, dried mixed wood sawdust biochar (MWSB) was degassed for 3 h at 200 °C before analysis. Following ASTM standard D6556–19 for multi-point BET analysis, the degassed sample was placed into the BET analyzer and subjected to the adsorption/desorption procedure for analysis. An energy-dispersive spectroscopy (EDS) equipped field emission scanning

Table 1
Lists of the kinetic models used to calculate the kinetic parameters.

KAS	$\ln\left(\frac{\delta}{T^2}\right) = \ln\left[\frac{AE}{Rg(x)}\right] - \frac{E}{RT}$ (5)
DAEM	$Ln\left(\frac{\delta}{T^2}\right) = \ln\left(\frac{AR}{E}\right) + 0.6075 - \frac{E}{RT}$ (6)
VZ	$\Phi(E_\alpha) = \sum_{i=1}^{n}\sum_{j\neq 1}^{n}\frac{I(E_\alpha, T_{\alpha,i})\beta_j}{I(E_\alpha, T_{\alpha,j})\beta_i}$ (7)
	The temperature integral is given as.
	$I(E_\alpha, T_\alpha) = \int_{T_{\alpha-\Delta\alpha}}^{T_\alpha} \exp\left(\frac{-E_\alpha}{RT}\right) dT$ (8)

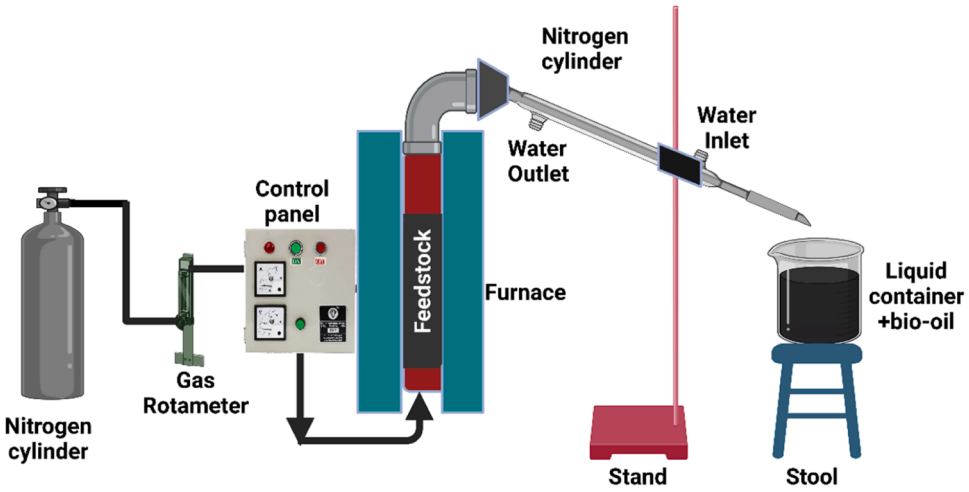

Fig. 1. Diagrammatic depiction of the experimental setup for pyrolysis.

electron microscope (FE-SEM) was used to evaluate the surface morphology. Carbon tape was put on the SEM tab, and a small amount of moisture-free biochar was spread on its surface (carbon tape serves as the background). An accelerating voltage of 15 kV was utilized to record the image, and the biochar was employed uncoated. In addition, the water holding capacity (WHC) was measured using the ceramic Buchner funnel, filter paper (size P8; Fisher brand), and deionized water.

3. Results and discussion

3.1. Physicochemical characterization of feeds

Table 2 lists the current findings from the proximate, ultimate, and compositional analyses of MWS and compares them with available studies of Acacia timber sawdust (ATD) [29], Sal wood sawdust [30], *Pinus halepensis* Mill. (PHC), and *Pinus Pinea* L. (PPC) [31]. MWS obtained moisture content (8.82 %), which was discovered to be less than the *Acacia timber* sawdust and higher than the other biomass listed in Table 2. Since biomass's initial moisture content was less than the permitted limit (<10 %), it should be favoured for thermal utilization because it proved to be a great feedstock for the generation of energy [32]. The moisture content in biomass significantly influences pyrolysis efficiency and product yield. High moisture levels reduce the thermal energy available for pyrolysis, leading to lower biochar yield and increased energy consumption for drying. Additionally, it can impact the quality of the bio-oil and gases produced, as excess water may lead to unwanted reactions during the process [32]. Higher levels of moisture in biomass demand an additional drying unit, which ultimately increases energy consumption and process costs. The volatile matter (VM), ash content, and fixed carbon of MWS were found to be 73.34 %, 6.59 %, and 11.25 %, respectively. The obtained volatile matter of MWS has a lower value than Sal Wood Sawdust but higher than other reported biomass in Table 2. Further, the ash content of MWS was found to be very close to *Pinus Pinea* L. (PPC) but higher than the *PHC* and SSD. Higher ignition of fuel during pyrolysis is indicated by the presence of more volatile matter and less ash [33]. Furthermore, increased volatile matter contributes to pyrolysis's ability to yield more bio-oil. In addition to VM, additional factors that affect the conversion of VM into bio-oil and gas include temperature, reaction time, and heating rate [34]. A high ash level is undesirable since it negatively impacts the combustion and gasification processes rather than aiding in the production of energy. The ash content is also affected by the kind of soil in the planted area and the presence of irrigation water [35]. The biomass has a higher ash content, works as a heat sink and decreases the overall heating value of fuel (Mishra & Mohanty, 2018a). During combustion, biomass with a higher ash content absorbs heat that would be used to burn fuel. Because of this, there is less energy accessible to conversion, which lowers the fuel's overall heating value and decreases the efficiency of the combustion process in producing energy. Additionally, the higher ash concentration of biomass causes salts to develop, which might shatter boilers or pipes. Further, fixed carbon in biomass is a crucial factor in pyrolysis as it directly influences the yield and quality of the resulting biochar. Higher fixed carbon content typically leads to greater biochar production, which is valued for its energy density, stability, and potential use as a carbon-rich soil amendment or adsorbent [32]. The elemental analysis of MWS confirmed 46.66 % carbon, 6.60 % hydrogen, 44.78 % oxygen, 1.32 % nitrogen, and 0.64 % sulfur, respectively. The amount of carbon content was found to be lower than

Table 2
Physiochemical characterisation of MWS along with other biomass and plastic waste.

Analysis	Mixed Wood Sawdust (MWS)	Acacia timber sawdust (ATD) [29]	Pinus halepensis Mill. (PHC) [31]	Pinus Pinea L. (PPC) [31]	Sal Wood Sawdust (SSD) [30]
Proximate analysis (dry basis, wt.%)					
Moisture	8.82 ± 1.56	9.65	2.64	4.01	6.04
Volatile matter	73.34 ± 1.10	68.45	72.94	64.37	76.03
Ash content	6.59 ± 1.12	1.33	3.49	6.73	2.02
Fixed carbon	11.25 ± 0.02	20.56	20.92	24.89	15.99
Elemental analysis (dry basis, wt.%)					
C	46.66	47.40	57.60	54.53	50.43
H	6.60	5.91	7.18	6.56	5.99
O	44.78	45.27	30.51	31.14	43.06
N	1.32	1.30	0.78	0.94	0.52
S	0.64	0.12	0.45	0.09	-
H/C	1.70	1.49	1.50	1.44	1.42
O/C	0.71	0.72	0.40	0.43	0.67
Heating value (MJ/kg)	16.23 ± 0.04	19.53	23.70	22.33	19.18
Bulk density (kg/m^3)	185.36 ± 1.21	-	-	-	330.12
Compositional analysis (wt. %)					
Hemicellulose	21.34 ± 0.18	-	24	17.90	16.23
Cellulose	48.04 ± 0.14	-	51.90	49.10	49.52
Lignin	10.23 ± 0.11	-	21.90	31.60	13.20

the biomass in Table 2, possibly a difference in the biochemical composition of biomass. However, hydrogen content was found to be higher than ATD and SSD but lower than PHC and PPC. Also, oxygen content was found to be higher than PHC, PPC, and STD and lower than ATD. The amount of nitrogen content was found to be very close to ATD but higher than PHC, PPC, and SSD. The sulfur content was also found to be higher than all the listed biomass in Table 2. However, sulphur content was found to be in the range. The disparities in biomass content led to variations in the elemental composition. The carbon content in biomass is critical during pyrolysis as it determines the efficiency of carbon conversion into biochar. Higher carbon content leads to increased biochar yield and enhances its quality, making it more suitable for applications like soil amendment and carbon sequestration [32]. The hydrogen and oxygen content in biomass significantly affects the composition and quality of pyrolysis products. High hydrogen content favours the production of bio-oil and gases. In contrast, higher oxygen content can lead to lower energy density in bio-oil and increased production of water and CO_2, reducing the overall efficiency of the process [36]. In addition, a higher oxygen level lowers the heating value, and a lower oxygen content is typically preferable for producing high-quality bio-oil. Nitrogen and sulfur content in biomass are important in pyrolysis due to their impact on the environmental and chemical properties of the products. High nitrogen content can lead to the formation of toxic nitrogenous compounds in bio-oil. In contrast, sulfur content can produce harmful sulfurous emissions and reduce the quality of biochar, limiting its use in certain applications [36]. One of the greatest methods for verifying the atomic ratio in substances is the Van-Krevelen diagram. PHC, PPC, SSD, and ATD were found to have atomic ratios that were matched with MWS and documented in Fig. 2. The H/C and O/C ratios of any carbon-based fuel demonstrate the burning efficiency of fuel. A greater H/C ratio is preferred over an O/C ratio for optimum utilisation of biomass in a thermal process [37]. Table 2 shows that MWS has a hydrogen-to-carbon ratio (H/C) of 1.70, which is in good accord with the biomass that is listed in Table 2. MWS has an oxygen-to-carbon ratio of 0.71, which is comparable to the biomass shown in Table 2. The variation in the chemical structure (elemental and fiber content assessment) was the primary cause of the discrepancy in the atomic ratios of all the biomass reported. One crucial stage in proving biomass's suitability for pyrolysis is biochemical evaluation. HHV of MWS was determined to be 16.23 MJ kg^{-1}, which is less than the value listed in Table 2 for the other kinds of biomass. A higher HHV in biomass indicates energy can be released during pyrolysis, leading to greater efficiency and higher quality bio-oil and gas production, making the process more economically viable [36]. Additionally, it was discovered that MWS has a bulk density of 185.36 kg m^{-3}, which is less than SSD. The bulk density of biomass is significant in pyrolysis as it affects the material handling, reactor loading, and heat transfer efficiency. Higher bulk density allows for more biomass to be processed per unit volume, improving the overall efficiency of the pyrolysis process and reducing transportation and storage costs [36,38]. The main structural elements of biomass are cellulose, hemicellulose, and lignin, each of which has a unique function during pyrolysis. Due to its high glucose content, cellulose mostly aids in the production of gasses and bio-oil. Lower temperature-dependent hemicellulose affects volatile compound synthesis and increases the output of bio-oil. The most thermally stable ingredient, lignin, is principally responsible for the creation of biochar because of its intricate aromatic structure. The distribution and quality of pyrolysis products are determined by the relative amounts of these ingredients, which also influence the process's overall efficiency and intended result [36,38]. The results confirmed that MWS has 21.34 % hemicellulose, 48.04 % cellulose, and 10.23 % lignin, respectively, which aligns with the biomass reported in Table 2.

3.2. FTIR study

The relationship between wavenumber and transmittance is studied using FTIR for MWS, and the obtained spectra are shown in Fig. 3. In general, the FTIR analysis revealed the presence of significant alkanes, ethers, alkenes, esters, and aromatic derivatives. Primarily found in biomass are acids, phenols, aromatics, and humidity, which are all validated at peak 3450 cm^{-1} by -OH stretching vibration [39]. Additionally, peak 2883 cm^{-1}, which is associated with C-H bending, releveled the prevalence of lignin and carbohydrates [40]. Additionally, band peaks 1645–1551 cm^{-1} indicate the emergence of aromatics and confirmed alkenes that have been assigned with C=C [41,42]. The band peak 1442 cm^{-1} supported the C≡C deformation vibration, which identified the ether and ester in biomass as well as the survival of alkyne and C=O stretching [43]. The infrared band peak at 1059 cm^{-1} supported the stretching vibration of aromatic C-O bonds, while the band peak below 802–608 cm^{-1}, which reflects the C-H deformation of aromatic groups, showed low intensity because it might be associated with π-electron bonds [41,42].

3.3. XRD study

The complete set of biomass XRD pattern data is displayed in Fig. 4. It is difficult to determine the crystallinity of cellulose in a material. The shift in the inter-hydrogen bond caused cellulose's crystalline structure to be significantly changed. The main factor affecting the temperature at which decay occurs and the creation of liquid intermediates is

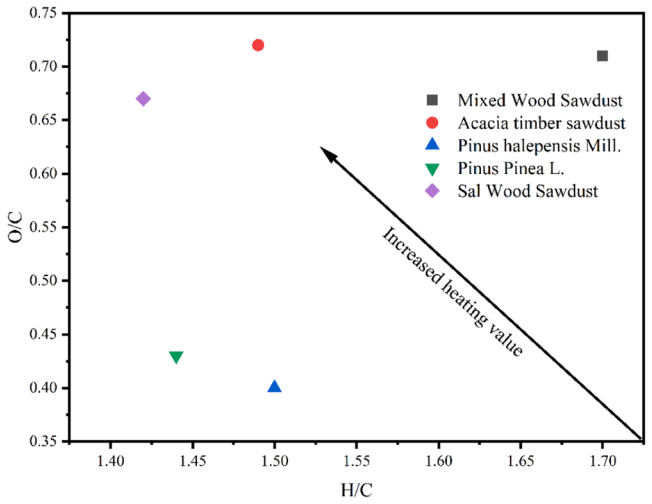

Fig. 2. Van Krevelen diagram MWS with other reported biomass.

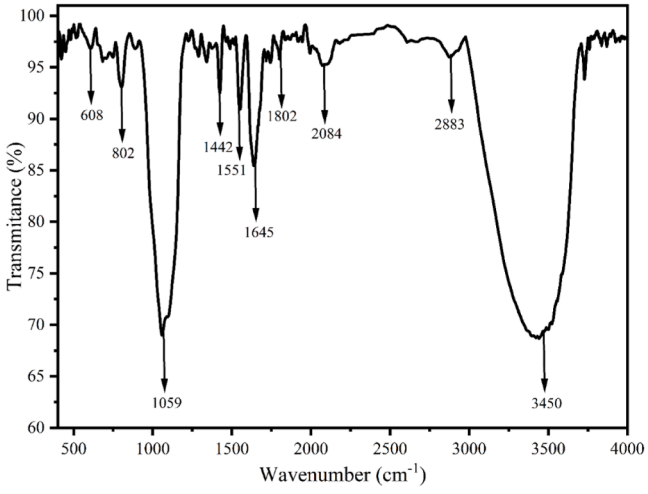

Fig. 3. Functional group estimation of MWS using FTIR analyser.

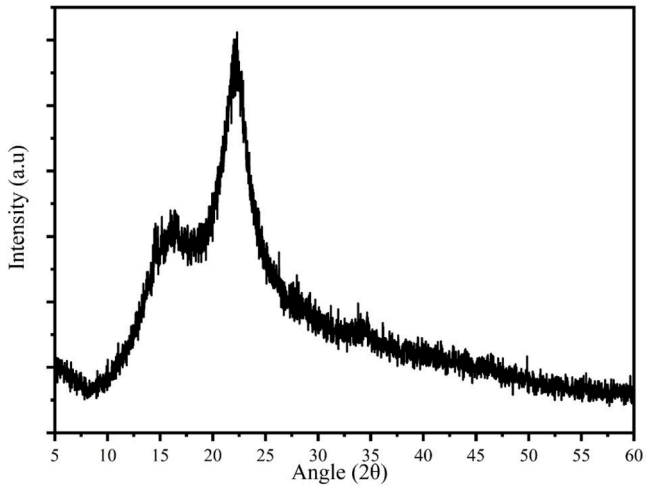

Fig. 4. XRD analysis of MWS.

cellulose's crystallinity. The reduced rate of depolymerization, apparent activation energy, and crystallinity dropdown thermal degradation temperature. As a result, the biomass needs to be examined using XRD before starting any pre-treatment. The high molecular mass hydrocarbons and specific fatty acid constituents that make up the wax have an impact on the crystallinity of biomass [44]. MWS did not exhibit a discernible upper peak in Fig. 4, suggesting an amorphous phase. After calculating the crystallinity index of the feed, biomass MWS was found to have higher indexes (40.51 %). The MWS crystallinity indices showed significant differences from other biomass that was reported (43–61.90 %), including rice straw, rice husk, cotton stalk, wheat straw, bagasse, maize stover, sorghum stalk, mustard stalk, corn cob, and Jatropha pruning [45,46].

3.4. Thermal stability study and effect of heating rate on biomass profile

A thermogravimetric analyzer (TGA) is used to study the thermal degradation profile of MWS, and Fig. 5(a) and (b) display the TGA and DTG thermograph against temperature at a heating rate of 10 °C min^{-1}. The weight of the sample decreased steadily but unevenly as the temperature rose (Fig. 5(a)), which shows three distinct phases that can be related to variations in the structure of the biomass's thermal stability. Stage 1 (up to 150 °C) causes the biomass to lose up to 10.51 % of its weight by removing most of its bound and unbound moisture as well as some light volatile organic compounds. Furthermore, because of the decomposition of hemicellulose, cellulose, and some lignin, stage 2, often referred to as the active pyrolysis stage (150–550 °C), experiences a large weight reduction (up to 73.34 %). Hemicellulose breaks down at lower temperatures of 100–300 °C because of its poor thermal endurance and less polymerization than cellulose and lignin. The breakdown of cellulose causes weight loss to increase in the 300–550 °C temperature range [47]. Two processes are involved in the breakdown of cellulose. The connections break into polymers at lower temperatures (up to 300 °C), producing carbon dioxide, carbon monoxide, and other carbonaceous gases. Moreover, in the second approach, bond integration produces liquid at very high temperatures (>300 °C). The biomass's residual lignin undergoes a gradual breakdown in the third step, or passive pyrolysis stage, which occurs at temperatures higher than 550 °C [12]. Lignin heat degradation occurs gradually at temperatures between 100 and 700 °C or higher. It is the greatest thermally resistant section of biomass at this stage and is what produces char due to its intricate structure of aromatic rings [12]. A similar thermal decomposition profile was also reported for rice husk (RH), rice straw (RS), wheat straw (WS), sugarcane bagasse (SB), arhar stalk (AS) and banana trunk (BT) [48]. The first step of MWS's DTG profiles (Fig. 5(b)) showed that the

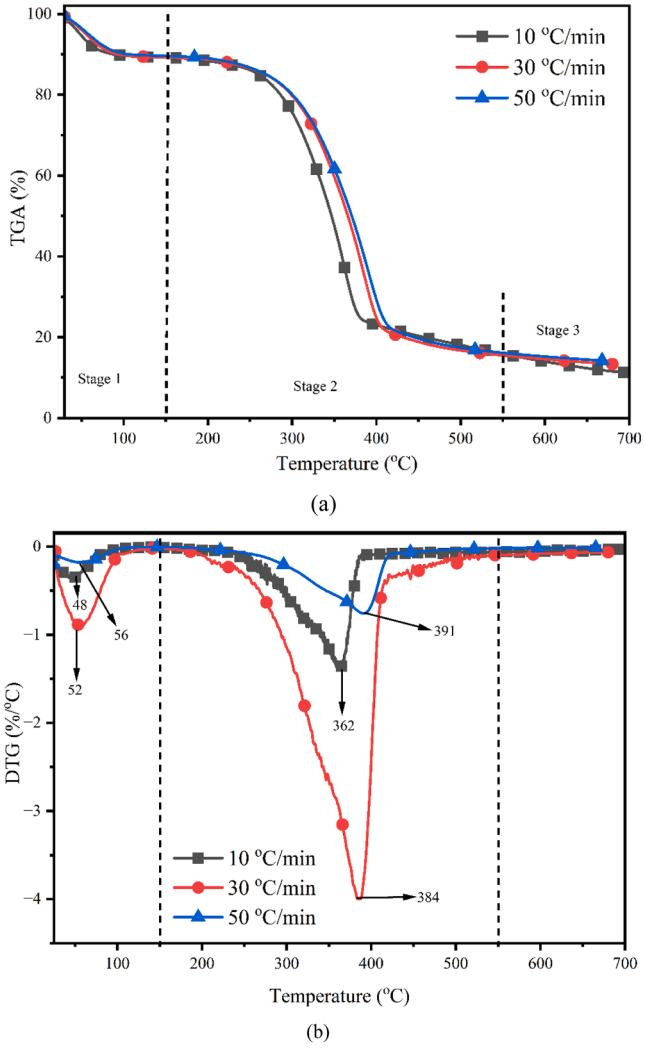

Fig. 5. Thermal profile study of MWS (a) weight loss profile, (b) derivative of weight loss profile at dynamic heating rates.

biomass had been cleared of specific light volatile organic components as well as unbound and bonded moisture. A peak that emerged at 48 °C suggested that some light volatile organic chemicals and unbound and bonded moisture had been abstracted. Moreover, the peaks at 362 °C indicated the breakdown of cellulose because of constant heat application, which resulted in 73.34 % weight loss. Lastly, in the final step, lignin breaks down more slowly (>550 °C), causing a 4.63 % reduction in body weight.

The effect of heating rates on the decomposition profile of MWS at dynamic heating rates (10, 30, and 50 °C min^{-1}) was studied and presented in Fig. 5(a and b). It was noted that by increasing the heating rates from 10–50 °C min^{-1}, the thermal decomposition profile of cellulose shifted towards a higher temperature zone (362, 384, and 391 °C), respectively. The fact that wood is a poor heat conductor and may create a thermal lag, or temperature gradient, throughout its cross-section could be one explanation for the change in the TGA curve. As long as adequate time is allowed for heating, the inner core of the biomass reaches the same temperature at a certain period at the lower heating rate, with the temperature profile along the cross-section of the biomass considered to be linear as the outer surface [49]. However, as the heating rate increases, there is a noticeable change in the temperature profile between the inner and outer cores of the biomass cross-section [50]. The other potential cause could be the impact of the heating rate of the subsequent reactions of the primary pyrolysis

products, namely tar and high molecular weight compounds. Further, better heat transfer occurs inside particle surfaces at lower heating rates [51]. Komandur et al. (2022) studied the pyrolysis kinetics of *Mesua ferrea* L., oilseed in a TGA using 5, 10, 20, and 40 °C min^{-1}, respectively [51]. They reported that by increasing heating rates, the thermal profile of biomass shifted 242, 253, 277.20, and 300.45 °C, respectively. Further, Samuelsson et al. (2015) stated that the TGA curve migrated to higher temperature zones of 340, 355, 368, 376, and 381 °C, respectively, with increasing heating rates (2, 5, 10, 15, and 20 °C min^{-1}), on Norway spruce biomass [52]. The results of the present investigation indicated that for heating rates between 10–50 °C min^{-1}, the overall volatile conversion in the active zone (second stage) was found to be 73.34, 73.77 and 73.84 % as the heating rate increased. The results showed that while total volatile products boosted with increasing heating rate, volatiles at lower heating rates remained in the reactor longer due to longer residence times. This longer residence time encouraged the development of secondary reactions like cracking, re-polymerization, and re-condensation, which again resulted in the formation of char [51]. Due to the complex kinetics of the biomass breakdown reaction, the barrier may form at lower heating rates. However, at greater heating rates, resistance may be overcome by increased mass and heat transmission between the particles, which again increases conversion [52]. Nonetheless, the TGA curve indicates that solid residue decreased (4.63, 2.14, and 1.87 %, respectively) consecutively as the heating rate increased from 10–50 °C min^{-1}. Increasing the heating rate from 10 to 50 °C min^{-1} accelerates the decomposition pattern of biomass. This rapid heating causes less time for thermal reactions, leading to quicker volatilization of the biomass components (like cellulose, hemicellulose, and lignin). As a result, more material is converted into gases and liquids rather than remaining as solid residue (char), leading to a decrease in the amount of solid remaining in the TGA [52].

3.6. Kinetic study

The pyrolysis reaction kinetics of MWS determines the activation energy using Kissinger-Akahira-Sunose (KAS), Distributed Activation Energy Model (DAEM), and Vyazovkin model (VZ) over conversion value, which is given in Table 3. The smallest amount of energy required to initiate a reaction is known as the activation of energy. A greater activation energy value indicates a slower reaction. The reactivity of the fuel is determined using the activation energy, which is vital to the pyrolysis system [53]. It reveals the creation and design of a new pyrolyzer in addition to optimising process parameters. From the results, the conversion values greater than 0.8 did not fit the data when the model was being fitted due to the poor correlation value [54]. KAS, DAEM, and VZ yielded average kinetic energy values of 234.06, 234.11, and 224.75 kJ mol^{-1}, respectively. Each model has a correlation coefficient greater than 0.95, indicating a value that best fits the experimental data. Additionally, it was noticed that activation energy varies with conversion, suggesting a high possibility of a multi-step reaction [54]. Model fitting was performed using the TGA experiment's data. It was found that the reduced correlation coefficient and conversion values of more than 0.8 are not appropriate for model fitting. KAS, DAEM, and VZ models yielded varying energy activation values of 268.36–220.71, 253.83–204.78, and 143.37–214.30 kJ mol^{-1}, respectively. The mechanism of the pyrolysis reaction determines the activation energy. A greater activation energy value indicates a slower reaction. Since pyrolysis is a continuous process and the activation energy is correlated with the heating rate, it follows that if the temperature rises, volatilization will also increase because of heat transfer between biomass particles. Fig. 6 shows the change in activation energy as a function of conversion value and standard deviation. The composition of biomass is dependent on the soil conditions in the growing area, and each biomass component has a unique breakdown temperature. Kinetic energy is a function of temperature. Consequently, one potential explanation could be a small fluctuation in the activation energy of biomass. Experimental setup, fuels, and mathematical calculations also influence activation

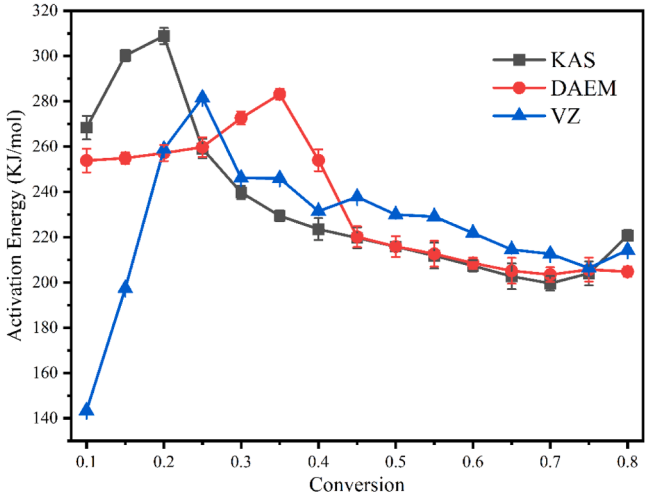

Fig. 6. Variation of activation energy against conversion value using KAS, DAEM, and VZ model.

Table 3
Kinetic analysis of biomass using KAS, DAEM, and VZ model.

Conversion	KAS			DAEM			VZ	
	Activation Energy KJ/mol)	R^2	Frequency factor (1/min)	Activation Energy (KJ/mol)	R^2	Frequency factor (1/min)	Activation Energy (KJ/mol)	Error
0.1	268.36	0.9199	4.60719E + 28	253.83	0.9939	1.46358E + 19	143.37	0.0075
0.15	300.27	0.9922	1.01549E + 25	254.93	0.9522	5.43831E + 18	197.41	0.0015
0.2	308.84	0.9788	2.09166E + 24	257.15	0.9978	3.20102E + 18	258.89	0.00047
0.25	259.12	0.9821	4.72784E + 18	259.80	0.9907	2.3952E + 18	281.59	0.0196
0.3	239.70	0.9862	3.18559E + 16	272.64	0.9927	8.52897E + 18	246.12	0.0092
0.35	229.41	0.9890	4.31123E + 15	283.14	0.9748	1.15986E + 20	245.94	0.0329
0.4	223.53	0.9908	5.83462E + 14	253.95	0.9798	3.03807E + 15	231.46	0.0144
0.45	219.72	0.9918	7.8963E + 13	220.15	0.9705	7.8963E + 13	237.76	0.0144
0.5	215.81	0.9917	2.90488E + 13	215.87	0.9974	3.21039E + 13	229.95	0.172
0.55	211.84	0.9924	1.06865E + 13	212.62	0.9755	65,659,969.14	229.09	0.0064
0.6	207.38	0.9936	3.93133E + 12	208.53	0.9791	3.93133E + 12	221.81	0.0081
0.65	202.70	0.9948	5.32048E + 11	205.14	0.9820	1.44626E + 12	214.53	0.01
0.7	199.58	0.9958	5.32048E + 11	203.44	0.9849	5.32048E + 11	212.60	0.0038
0.75	204	0.9973	1.9573E + 11	205.68	0.9884	5.32048E + 11	206.35	0.0049
0.8	220.71	0.9999	1.06865E + 13	204.78	0.9993	1.68902E + 10	214.30	0.0011
Average	**234.06**		**3.07227E + 27**	**234.10**		**1.00126E + 19**	**224.75**	

energy.

3.7. Physicochemical characterisation of biochar

Table 4 lists the physicochemical characteristics of the biochar that was formed at various temperatures. Table 4 demonstrates that the biochar yield decreased by around 19 % as the pyrolysis temperature increased from 400–900 °C because of the increased biomass volatilization. Raising the pyrolysis temperature from 400 °C to 900 °C results in a decrease in biochar yield because the destruction of organic matter is accelerated into volatile chemicals that are emitted as gases at higher temperatures. Consequently, a reduced yield of biochar is produced since less solid carbonaceous material is left behind. Higher temperatures further accelerate the carbonisation process, which further reduces the biochar's bulk [55]. At low temperatures, a greater yield was produced with minimal loss of aliphatic fractions and surface functional groups, such as H and O. The loss of hydroxyl groups as a result of dehydration, cellulose, and hemicellulose's thermal breakdown led to a low biochar output [56]. Further, the moisture content of biochar was found to be slightly decreased by increasing the pyrolysis temperature from 400–900 °C (Table 4). The moisture content of biochar decreases with increasing pyrolysis temperature because higher temperatures drive off more water and volatile compounds from the biomass, resulting in drier and more stable biochar with lower residual moisture [55]. The ash content of biochar was also found to be increased by 4.84 % by increasing the pyrolysis temperature from 400–900 °C. The ash concentration of biochar rises as the pyrolysis temperature rises because the organic parts of the biomass volatilize and break down at higher temperatures, leaving behind inorganic minerals such as ash. These minerals settle to the bottom of the remaining biochar because they are not volatile [57]. The elemental analysis of biochar revealed that raising the pyrolysis temperature raised the carbon content. This came about as a result of high temperatures and high degrees of carbonisation in aromatic substances [53]. On the other hand, the loss of nitrogen, oxygen, and hydrogen was noted simultaneously. The breakdown of weak bonds within the material's structure at high pyrolysis temperatures has been attributed to hydrogen and oxygen loss [58]. The carbonisation process was blamed for the removal of water, hydrocarbons, tarry fumes, H_2, CO, and CO_2 [58]. Biochar was discovered to contain nitrogen at lower temperatures (400 °C), but as the temperature was raised to 600–900 °C during the pyrolysis process, more volatile components were lost, and the nitrogen content vanished [58]. The HHV of biochar was raised by 5.72 % by raising the pyrolysis temperature from 400 to 900 °C due to the increased elemental composition of biochar. The measured result is consistent with biochar made from Samanea saman seeds (23.14 MJ kg^{-1}) [59]. The presence of HHV in biochar suggests that it is capable of being utilised as a solid fuel for cooking and home heating [60]. Furthermore, the acidity of the biochar rose due to proton ions were eliminated in terms of moisture when the pyrolysis temperature was raised [56]. It was discovered that raising the pyrolysis temperature from 400–900 °C enhanced the bulk density of the biochar (Table 4). As the temperature of pyrolysis rises, the combustible stuff burns and the density of biochar increases [61]. The BET surface area of biochar demonstrated a reduction in BET surface area by 17 % when the temperature was raised from 400 to 900 °C. The BET surface area of biochar can decrease with increasing pyrolysis temperatures from 400 °C to 900 °C due to the collapse or sintering of micropores at higher temperatures [62]. At elevated temperatures, the intense thermal energy can cause the structure of the biochar to become more condensed, reducing the overall pore volume and surface area. Additionally, excessive carbonisation can close off pores, further decreasing the accessible surface area [62]. One crucial parameter that highlights biochar potential is water-holding capacity (WHC). The WHC of biochar is lowered by raising the pyrolysis temperature from 400 to 900 °C. As pyrolysis temperatures rise from 400 °C to 900 °C, the amount of water that biochar can hold decreases because the structure of the material becomes less porous and more condensed at higher temperatures. This decrease in pore volume and surface area limits the biochar's capacity to absorb and hold water. The hydrophilic functional groups on the surface of biochar can also be reduced by high temperatures, which would further lessen the material's attraction to water [63].

Table 4
Physicochemical characterisation of char obtained from the pyrolysis at diffrent.

Analysis	MWSB400	MWSB600	MWSB900
Yield (wt.%)	34.5 ± 0.11	24.45 ± 0.14	15.48 ± 0.16
Proximate study (wt.%) on a dry basis			
Moisture	5.82 ± 0.21	5.18 ± 0.60	4.62 ± 0.80
Ash content	11 ± 0.14	16.32 ± 0.12	18.94 ± 0.12
Elemental study (wt.%, on dry basis)			
C	66.46	75.18	76.02
H	5.59	4.27	1.97
O	26.95	20.32	22.01
N	1	0.23	-
S	-	-	-
HHV (MJ/kg)	31.25 ± 0.10	32.18 ± 0.20	36.97 ± 0.20
pH	4.94 ± 0.10	6.97 ± 0.10	9.07 ± 0.10
WHC (wt.%)	34.45 ± 1.60	33.52 ± 1.41	28.45 ± 1.10
Bulk Density (kg/m^3)	172.68 ± 1.40	188.69 ± 1.15	205.11 ± 1.67
BET surface area (m^2/g)	79.58± 1.10	71.20 ± 1.12	62.58 ± 1.11

3.8. FTIR study of Biochar

The biochar produced at dynamic temperatures was examined by the functional group through the use of an FTIR analyser and is illustrated in Fig. 7. The results showed that biochar's structural properties differ significantly when the pyrolysis temperature is raised and the holding time is extended. The presence of halocarbon compounds, including organofluorine, organochlorine, organobromine, and organoiodine, is revealed by the observed peak at a wavelength of below 900 cm^{-1}, which is attributable to C-X stretching vibration [64]. The band peak in the 1000–1200 cm^{-1} range was attributed to C-O stretching originating from hemicellulosic groups such as lactone and quinine. A decrease in the strength of the C-O stretch, a sign of hemicellulose breakdown, was noted when the pyrolysis temperature was raised from 400 to 800 °C [53]. It was discovered that increasing the temperature reduced or even eliminated carboxylic acids and that biomass pyrolysis clearly broke down hemicellulosic materials [64]. The band peaks between 1350 and 1600 cm^{-1}, and the stretching vibrations of CH_2 and -OH from the breakdown of phenol are responsible for this. Additionally, the band peak spanning 1900–2300 cm^{-1} revealed CO_2 molecules [56]. Further, at 2974 cm^{-1}, a very weak aliphatic (C-H stretching) signal indicated the presence of cellulose and hemicellulose [56]. The bond peaks detected

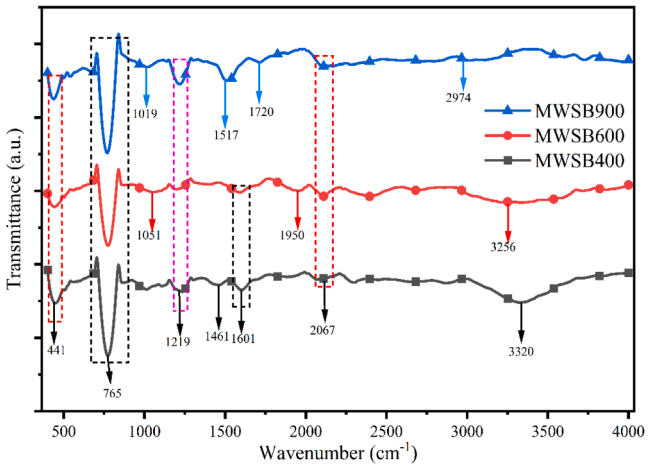

Fig. 7. FTIR study of biochar obtained at 400, 600, and 900 °C.

between 3430 and 3450 cm^{-1}, which were ascribed to the -OH stretching vibration, indicated the presence of phenolic components, acids, and moisture. Nonetheless, it would be anticipated that consistently raising the pyrolysis temperature over 900 °C might eliminate the problem; as the temperature rises, the dehydration reaction gets better and eliminates moisture and acid through the aromatisation process [53]. The method of producing biochar begins with the degradation of lignocellulose due to a free radical mechanism known as thermal hemolytic breaking of bonds between biomass's structured oxygen and inorganic components. The overall increase in pyrolysis temperature changed the existing functional groups, leading to dehydration of ligneous and cellulosic components and reduced aliphatic molecules. This demonstrates that the molecular and dipole connections between moisture and biochar were enhanced at higher temperatures, increasing the biochar's acidity [65].

3.9. XRD study of biochar

The structure of biochar is shown in Fig. 8 based on the XRD study. Using existing research and Match software (Crystal Impact, Germany), the peak is identified. Biochar made by slowly pyrolyzing MWSB at 400, 600, and 900 °C for 45 min is used for the XRD examination. The XRD analysis revealed a wide range of mineral crystals and other inorganic components (Fig. 8). It was observed that a number of peaks overlapped and offered a variety of possible peak combinations. The figure near the reference points was assigned to that peak because the examination was primarily qualitative rather than quantitative. The peak described at 22.51, 23.40 and 24.81° suggested the presence of graphite, fluorite, and chlorapatite, respectively, may have been present [64]. Further, Gibbsite was found by increasing the pyrolysis temperature from 400 to 900 °C, which resulted in the discovery of a second, more intense peak at 22.51–24.81°. Moreover, the comparatively low intensities of peaks linked to hydrobiotite, bayerite, and calcite were found. Graphite and fluorite were also observed, along with a few more peaks that corresponded to apophyllite, pyrophyllite, and barite at 29.25, 29.41, 35.21, 43 and 43.10°, respectively [64]. When the pyrolysis temperature was raised to 900 °C, new peaks of a particular intensity formed and the detected firm peaks in the XRD spectra of biochar produced at 400 °C vanished. There was a somewhat higher signal-to-noise ratio, a slightly more prominent background, and a considerably reduced variety of peaks and their intensities. The way that minerals break down at high temperatures and produce new elements was highlighted by this peak change. The sharp peak at 24.81° showed fluorite, while further high-intensity peaks at 35.21°, 43, and 43.10° were thought to include gibbsite and chlorite, respectively [64]. The more amorphous material could be the reason for the hump in the XRD spectra of biochar at 600 and 900 °C since rising temperatures would cause some of the constituents with thermal breakdown between 600 and 900 °C to disintegrate. The XRD data of all the biochar samples revealed a variety of mineral components, such as silicon, calcium, magnesium, sodium, iron, sulfur, and carbon. Overall, it was discovered that the temperature had a more considerable effect on the structural composition of the biochar. Yuan et al. (2011) report that as the temperature increased from 300 to 500 °C throughout the production process, the mineralogical heterogeneity of the biochar changed. Additional studies, including Waqas et al. (2018) [66], Ahmad et al. (2017) [67], and Ding et al. (2016) [68], observed that an increase in the pyrolysis temperature changed the amount of minerals of biochar.

3.11. Thermal stability of biochar

Fig. 9 shows the thermal degradation curve of MWSB at different temperatures (400, 600 and 900 °C). The biochar's TG profile suggested that the decomposition percentage significantly decreased when the temperature was raised from 400 to 900 °C. The TGA profile confirmed 46.98, 34.93 and 24.12 % decomposition of MWSB for 400, 600 and 900 °C, respectively. The biochar that has been pyrolysed at temperatures 900 °C has the highest thermal stability, meaning it may be utilised at higher temperatures. The biochar produced at a lower temperature (400 °C) decomposed maximum (46.98 %) due to the presence of combustible materials. Biochar produced at 400 °C decomposes more than at 600 and 900 °C because lower temperatures retain more volatile compounds and organic matter, making it less stable. Higher temperatures (600 °C and 900 °C) result in greater carbonization, producing more stable and resistant biochar with fewer volatiles [69]. Additionally, it was observed that biochar produced at 400, 600, and 900 °C displayed three-stage breakdown patterns. In the initial stage (30–100 °C), biochar produced at 400, 600, and 900 °C demonstrated 2.04, 11.92, and 11.11 % decomposition for MWSB. Additionally, MWSB in the second stage (100–450 °C) of the biochar generated at 400, 600, and 900 °C showed 17.03, 3.33, and 1.39, but in the third stage (550–900 °C), MWSB showed 27.96, 16.66, and 11.55 %, respectively. The first stage's weight loss results from the moisture and extremely light volatile materials being removed from the pores and surface of the biochar [61]. The biochar produced at 400 °C degraded most in the second and third stages because of incomplete biomass pyrolysis. The incomplete pyrolysis of biomass is referred to as partial pyrolysis. Because of problems with heat and mass transport, biomass did not completely break down at 400 °C. However, because of the adequate heat and mass transmission between the biomass particles, biochar produced at higher temperatures of 600

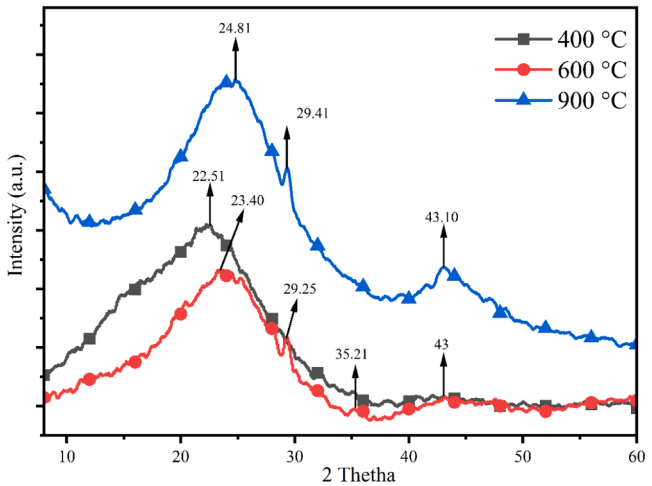

Fig. 8. XRD analysis of biochar obtained at 400, 600 and 900 °C.

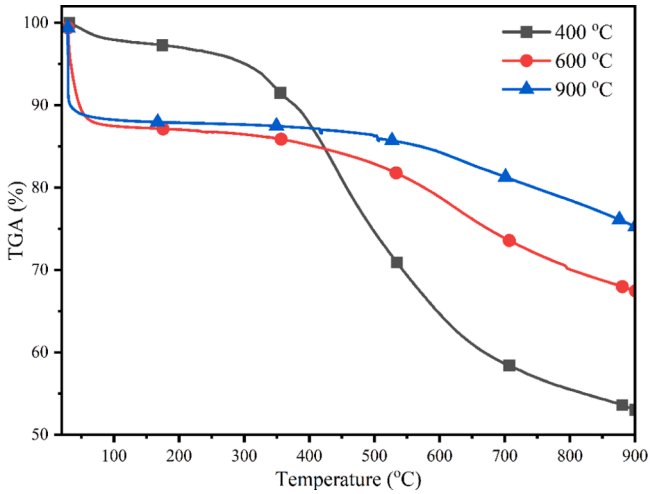

Fig. 9. Thermal stability profile of biochar at 400, 600 and 900 °C.

and 900 °C degraded minimally [30]. The breakdown of cellulose and hemicellulose at high temperatures has been connected to weight reduction [70]. The minor overlap between the hemicellulose and cellulose breakdown temperatures resulted in a curve rather than a distinct peak [71]. Furthermore, weight loss at higher temperatures was discovered to be less because lignin degradation requires greater temperatures than does the disintegration of carbohydrates [71]. The three biochar samples showed somewhat different patterns of heat deterioration from one another. The 900 °C biochar showed better thermal stability when compared to the other two biochar samples (400 and 600 °C). The increased temperature during pyrolysis most likely increased the thermal stability of the biochar by producing more stable carbon forms. During pyrolysis, the decomposition of lignocellulosic biomass was regulated by lignin, cellulose, and hemicellulose [71]. A similar decomposition profile of mixed waste biomass-derived biochar was reported by Suresh Babu et al. (2024) [25]

3.12. FESEM study of biochar

The morphology of biochar generated at different temperatures and after 45 min of holding time is shown **in** Fig. 10 (a, b and c). The results showed that increasing the temperature sped up the volatilization process and significantly altered the surface of the resultant biochar. As the temperature increased, the biochar's microparticles and micropores transformed the asymmetrical fold structure into a regular layer [53]. Numerous processes, including dehydration, decarbonylation, and decarboxylation, occur during pyrolysis and change the shape of biochar [72]. The organic components volatilised to generate biochar, which was synthesised at 400 °C and maintained for 45 min, as shown in Fig. 10 (a) [56]. This biochar has a slightly porous surface. The organic material burned during heat processing, resulting in the creation of pores. In terms of feedstock, biochar has a higher average porosity [65]. As the pyrolysis temperature was increased from 400 to 900 °C, flake-like structures began to form on the surface (Fig. 10 **b and c**). At 400 °C, produced biochar has a smooth surface and some macropores, whereas 600 and 900 °C produced biochar has an uneven surface topography. The flake texture of biochar generated at higher temperatures is caused by a phenomenon wherein micropores are occupied with tars (condensed volatiles) and other decomposition products that partially clog pores [64,70]. The pyrolysis caused the chemical connection to break, altering the pore size and structure of the biochar [73]. Fig. 10 **(a, b and c)** showed that varying the holding times had no discernible effect on the surface morphology.

4. Significance, limitations, and future scope

This present study is significant because it offers a detailed examination of how pyrolysis temperature affects the yield and properties of biochar, focusing on kinetic models (KAS, DAEM, VZ) for various biomass feedstocks. By evaluating the influence of temperature on biochar carbon content, thermal stability, and surface characteristics, the research provides insights into optimising pyrolysis for applications such as carbon sequestration, soil enhancement, and wastewater treatment. Understanding these effects is crucial for enhancing the quality and efficiency of biochar production, making it a more sustainable and valuable resource for environmental and industrial purposes. The limitation of the study is its focus on a limited set of temperatures and biomass types, which may not fully capture the diversity of feedstocks and operational conditions encountered in real-world applications. Additionally, while the kinetic models used (KAS, DAEM, VZ) are effective, they may not completely represent the complex nature of pyrolysis, such as the heterogeneous nature of the reaction or the influence of catalysts. The accuracy of model predictions, especially at higher conversions (>0.8), could be affected by the simplifications inherent in these models, which do not always account for all the nuances of the process. Future research could extend the study by considering a broader range of biomass feedstocks, including agricultural, forestry, and waste-derived materials. Further exploration of varying pyrolysis conditions, including different heating rates, pressures, and the role of catalysts, could improve biochar yield and quality. Integrating life cycle analysis and economic feasibility studies with

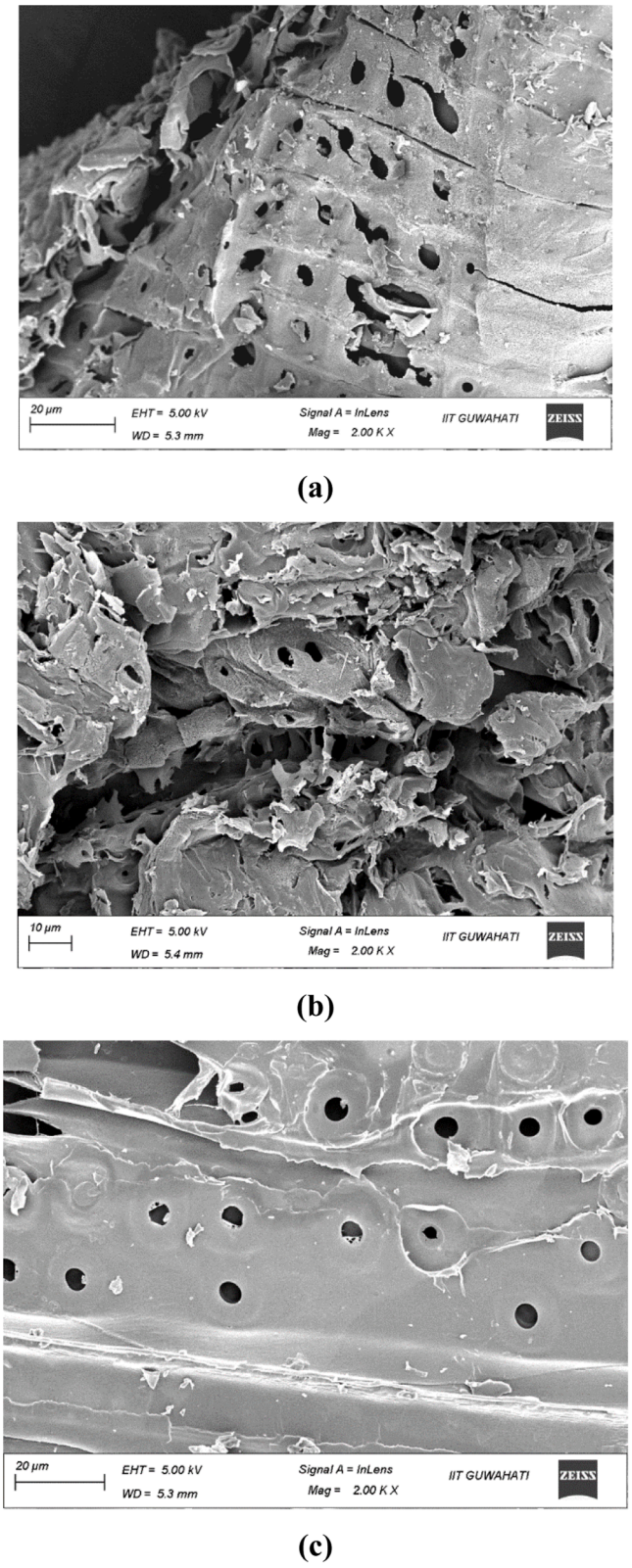

Fig. 10. FESEM analysis of biochar obtained at (a) 400, (b) 600 and (c) 900 °C.

kinetic and thermodynamic data will be essential for scaling up biochar production. Moreover, understanding the interaction between feedstock characteristics and temperature will be vital for tailoring biochar properties to specific applications in agriculture, energy, and environmental management.

5. Conclusions

The current study examines the physicochemical characterisation of mixed waste sawdust (MWS), pyrolysis kinetic behaviour, and biochar production using a slow pyrolysis technique. The current investigation also looked at the temperature effects on the yields and characteristics of biochar. The bioenergy potential of biomass for biochar generation was proven by its physicochemical characterisation results. Furthermore, the biomass kinetic analysis confirmed that a multifaction process rather than a single reaction was used to decompose the biomass. Moreover, the biomass's thermal profile verified the three-stage process, and the TGA profile of the biomass changed toward a higher temperature zone as heating rates were raised from 10 to 50 °C min^{-1}. Further, the pyrolysis of biomass confirmed the maximum biochar yield at 400 °C. Further, the yield of biochar decreased as the pyrolysis temperature rose from 600–900 °C due to the decomposition of biomass. The biochar obtained at 900 °C showed reduced oxygen content, an increased HHV, and higher carbon content. The biochar thermal profile shows that biochar produced at 900 °C is more thermally stable at higher temperatures than at 400 and 600 °C. Finally, the surface morphology of the biochar revealed that while biochar acquired at 400 °C can be utilized for fertiliser or soil applications, and biochar produced at 600 and 900 °C can be used for carbon-based applications.

Data availability

The datasets generated and/or analysed during the current study are not publicly available but are available from the corresponding author on reasonable request.

CRediT authorship contribution statement

Nikhill Rambhatla: Conceptualization, Data curation, Formal analysis, Investigation, Writing – original draft. **Tanushka Florence Panicker:** Conceptualization, Data curation, Formal analysis, Investigation, Writing – original draft. **Ranjeet Kumar Mishra:** Writing – review & editing, Visualization, Validation, Supervision, Software, Resources, Project administration, Investigation, Formal analysis. **Srinivas Kini Manjeshwar:** Project administration, Resources, Software, Validation, Writing – review & editing. **Abhishek Sharma:** Project administration, Resources, Software, Supervision, Validation, Visualization, Writing – review & editing.

Declaration of competing interest

The authors announce that they have no known competing financial interests or personal relationships that could have appeared to influence the work testified in this paper.

Acknowledgements

The author would like to thank the Biomass, bioenergy, biofuel and bioproducts lab, department of Chemical Engineering, Manipal Institute of Technology, Manipal, Karnataka, India, for providing the necessary facilities.

Data availability

Data will be made available on request.

References

[1] A.T. Koçer, B. Mutlu, D. Özçimen, Investigation of biochar production potential and pyrolysis kinetics characteristics of microalgal biomass, BioMass Convers. Biorefin. 10 (2020) 85–94.
[2] E. Emmanouilidou, A. Lazaridou, S. Mitkidou, N.C. Kokkinos, A comparative study on biodiesel production from edible and non-edible biomasses, J. Mol. Struct. 1306 (2024) 137870.
[3] A. Selvarajoo, D. Oochit, Effect of pyrolysis temperature on product yields of palm fibre and its biochar characteristics, Mater. Sci. Energy Technol. 3 (2020) 575–583.
[4] L. Adelard, T.G. Poulsen, V. Rakotoniaina, Biogas and methane yield in response to co-and separate digestion of biomass wastes, Waste Manag. Res. 33 (1) (2015) 55–62.
[5] R.S. Perumal, B. Muralidharan, Valorization of Ricinus communis outer shell biomass to biochar: impact of thermal decomposition temperature on physicochemical properties and EMI shielding performance, Results. Eng. 24 (2024) 103097.
[6] S. Yorgun, D. Yıldız, Slow pyrolysis of paulownia wood: effects of pyrolysis parameters on product yields and bio-oil characterization, J. Anal. Appl. Pyrolysis. 114 (2015) 68–78.
[7] J.A. Okolie, A. Mukherjee, S. Nanda, A.K. Dalai, J.A. Kozinski, Next-generation biofuels and platform biochemicals from lignocellulosic biomass, Int. J. Energy Res. 45 (10) (2021) 14145–14169.
[8] N.C. Kokkinos, E. Emmanouilidou, Waste-to-Energy: Applications and Perspectives on Sustainable Aviation Fuel production, Renewable Fuels for Sustainable Mobility, Springer, 2023, pp. 265–286.
[9] A. Pattiya, Catalytic pyrolysis, Direct Thermochem. Liquefact. Energy Appl. (2018) 29–64.
[10] M.A. Mehmood, G. Ye, H. Luo, C. Liu, S. Malik, I. Afzal, J. Xu, M.S. Ahmad, Pyrolysis and kinetic analyses of Camel grass (Cymbopogon schoenanthus) for bioenergy, Bioresour. Technol. 228 (2017) 18–24.
[11] B. Zhao, X. Xu, H. Li, X. Chen, F. Zeng, Kinetics evaluation and thermal decomposition characteristics of co-pyrolysis of municipal sewage sludge and hazelnut shell, Bioresour. Technol. 247 (2018) 21–29.
[12] J.E. White, W.J. Catallo, B.L. Legendre, Biomass pyrolysis kinetics: a comparative critical review with relevant agricultural residue case studies, J. Anal. Appl. Pyrolysis. 91 (1) (2011) 1–33.
[13] J. Nascimento, E. Camelo, M. Carvalho, C. Virgens, Kinetic evaluation of Pachira aquatica Aubl biomass slow pyrolysis towards to biochar production, Biofuels. 15 (6) (2024) 615–625.
[14] T.G. Ambaye, M. Vaccari, A. Bonilla-Petriciolet, S. Prasad, E.D. van Hullebusch, S. Rtimi, Emerging technologies for biofuel production: a critical review on recent progress, challenges and perspectives, J. Environ. Manage 290 (2021) 112627.
[15] R.K. Mishra, M. Misra, A.K. Mohanty, Value-added biocarbon production through slow pyrolysis of mixed bio-oil wastes: studies on their physicochemical characteristics and structure–property–processing co-relation, BioMass Convers. Biorefin. 14 (6) (2024) 7887–7901.
[16] N. Schmitt, A. Apfelbacher, N. Jäger, R. Daschner, F. Stenzel, A. Hornung, Thermochemical conversion of biomass and upgrading to biofuel: the Thermo-Catalytic Reforming process–a review, Biofuel. Bioproduct. Biorefining 13 (3) (2019) 822–837.
[17] A.A. Boateng, Pyrolysis of Biomass for Fuels and Chemicals, Academic Press, 2020.
[18] M. Gholizadeh, X. Hu, Q. Liu, A mini review of the specialties of the bio-oils produced from pyrolysis of 20 different biomasses, Renew. Sustain. Energy Rev. 114 (2019) 109313.
[19] M.d.C. Rangel, F.M. Mayer, M.d.S. Carvalho, G. Saboia, A.M. de Andrade, Selecting catalysts for pyrolysis of lignocellulosic biomass, Biomass 3 (1) (2023) 31–63.
[20] M. Afshar, S. Mofatteh, Biochar for a sustainable future: environmentally friendly production and diverse applications, Results. Eng. 23 (2024) 102433.
[21] H. Lyu, Q. Zhang, B. Shen, Application of biochar and its composites in catalysis, Chemosphere 240 (2020) 124842.
[22] J.J. Manyà, M. Azuara, J.A. Manso, Biochar production through slow pyrolysis of different biomass materials: seeking the best operating conditions, Biomass Bioenergy 117 (2018) 115–123.
[23] S.S. Sahoo, V.K. Vijay, R. Chandra, H. Kumar, Production and characterization of biochar produced from slow pyrolysis of pigeon pea stalk and bamboo, Clean. Eng. Technol. 3 (2021) 100101.
[24] S.G.C. de Almeida, L.A.C. Tarelho, T. Hauschild, M.A.M. Costa, K.J. Dussán, Biochar production from sugarcane biomass using slow pyrolysis: characterization of the solid fraction, Chem. Eng. Process. - Process Intensificat. 179 (2022) 109054.
[25] K.K.B. Suresh Babu, M. Nataraj, M. Tayappa, Y. Vyas, R.K. Mishra, B. Acharya, Production of biochar from waste biomass using slow pyrolysis: studies of the effect of pyrolysis temperature and holding time on biochar yield and properties, Mater. Sci. Energy Technol. 7 (2024) 318–334.
[26] J. Cai, L. Bi, Kinetic analysis of wheat straw pyrolysis using isoconversional methods, J. Therm. Anal. Calorim. 98 (1) (2009) 325–330.
[27] R.K. Mishra, K. Mohanty, Pyrolysis kinetics and thermal behavior of waste sawdust biomass using thermogravimetric analysis, Bioresour. Technol. 251 (2018) 63–74.
[28] R.K. Mishra, K. Mohanty, Kinetic analysis and pyrolysis behaviour of waste biomass towards its bioenergy potential, Bioresour. Technol. 311 (2020) 123480.
[29] A. Ahmed, M.S. Abu Bakar, R.S. Sukri, M. Hussain, A. Farooq, S. Moogi, Y.-K. Park, Sawdust pyrolysis from the furniture industry in an auger pyrolysis reactor system for biochar and bio-oil production, Energy Convers. Manage 226 (2020) 113502.
[30] R.K. Mishra, K. Mohanty, Pyrolysis of low-value waste sawdust over low-cost catalysts: physicochemical characterization of pyrolytic oil and value-added biochar, Biofuel Res. J. 9 (4) (2022) 1736–1749.

[31] A. Maaoui, A. Ben Hassen Trabelsi, A. Ben Abdallah, R. Chagtmi, G. Lopez, M. Cortazar, M. Olazar, Assessment of pine wood biomass wastes valorization by pyrolysis with focus on fast pyrolysis biochar production, J. Energy Inst. 108 (2023) 101242.
[32] J. Dong, Y. Chi, Y. Tang, M. Ni, A. Nzihou, E. Weiss-Hortala, Q. Huang, Effect of operating parameters and moisture content on municipal solid waste pyrolysis and gasification, Energy Fuels 30 (5) (2016) 3994–4001.
[33] S. Aich, D. Behera, B.K. Nandi, S. Bhattacharya, Relationship between proximate analysis parameters and combustion behaviour of high ash Indian coal, Int. J. Coal. Sci. Technol. 7 (4) (2020) 766–777.
[34] J. Cai, Y. He, X. Yu, S.W. Banks, Y. Yang, X. Zhang, Y. Yu, R. Liu, A.V. Bridgwater, Review of physicochemical properties and analytical characterization of lignocellulosic biomass, Renew. Sustain. Energy Rev. 76 (2017) 309–322.
[35] X. Yao, Y. Hu, J. Ge, X. Ma, J. Mao, L. Sun, K. Xu, K. Xu, A comprehensive study on influence of operating parameters on agglomeration of ashes during biomass gasification in a laboratory-scale gasification system, Fuel 276 (2020) 118083.
[36] T. Kan, V. Strezov, T.J. Evans, Lignocellulosic biomass pyrolysis: a review of product properties and effects of pyrolysis parameters, Renewable and sustainable energy reviews 57 (2016) 1126–1140.
[37] M. Kumar, P. Mishra, S. Upadhyay, Pyrolysis of Saccharum munja: optimization of process parameters using response surface methodology (RSM) and evaluation of kinetic parameters, Bioresour. Technol. Rep. 8 (2019) 100332.
[38] M. Morin, S. Pécate, M. Hemati, Y. Kara, Pyrolysis of biomass in a batch fluidized bed reactor: effect of the pyrolysis conditions and the nature of the biomass on the physicochemical properties and the reactivity of char, J. Anal. Appl. Pyrolysis. 122 (2016) 511–523.
[39] J.M. Jabar, Y.A. Odusote, Y.T. Ayinde, M. Yılmaz, African almond (Terminalia catappa L) leaves biochar prepared through pyrolysis using H3PO4 as chemical activator for sequestration of methylene blue dye, Results. Eng. 14 (2022) 100385.
[40] P. Doshi, G. Srivastava, G. Pathak, M. Dikshit, Physicochemical and thermal characterization of nonedible oilseed residual waste as sustainable solid biofuel, Waste Manag. 34 (10) (2014) 1836–1846.
[41] Y.-C. Lin, S.-H. Ho, Y. Zhou, N.-q. Ren, Highly efficient adsorption of dyes by biochar derived from pigments-extracted macroalgae pyrolyzed at different temperature, Bioresour. Technol. 259 (2018) 104–110.
[42] A. Ahmed, M.S.A. Bakar, A. Razzaq, S. Hidayat, F. Jamil, M.N. Amin, R.S. Sukri, N. S. Shah, Y.-K. Park, Characterization and thermal behavior study of biomass from invasive Acacia mangium species in Brunei preceding thermochemical conversion, Sustainability. 13 (9) (2021) 5249.
[43] O.R. Obanla, J.A. Hestekin, M.E. Ojewumi, I. Bousrih, M.C. Fawole, Enhancing rubber (Hevea brasiliensis) seed shell biochar through acid-base modification for effective phenol removal from aqueous environments, Results. Eng. 20 (2023) 101584.
[44] F. Domergue, M. Miklaszewska, The production of wax esters in transgenic plants: towards a sustainable source of bio-lubricants, J. Exp. Bot. 73 (9) (2022) 2817–2834.
[45] M. Dash, V. Venkata Dasu, K. Mohanty, Physico-chemical characterization of Miscanthus, Castor, and Jatropha towards biofuel production, J. Renew. Sustain. Energy 7 (4) (2015) 043124.
[46] T. Raj, M. Kapoor, R. Gaur, J. Christopher, B. Lamba, D.K. Tuli, R. Kumar, Physical and chemical characterization of various Indian agriculture residues for biofuels production, Energy Fuels 29 (5) (2015) 3111–3118.
[47] J.Y. Yeo, B.L.F. Chin, J.K. Tan, Y.S. Loh, Comparative studies on the pyrolysis of cellulose, hemicellulose, and lignin based on combined kinetics, J. Energy Inst. 92 (1) (2019) 27–37.
[48] M. Kumar, S.N. Upadhyay, P.K. Mishra, A comparative study of thermochemical characteristics of lignocellulosic biomasses, Bioresour. Technol. Rep. 8 (2019) 100186.
[49] A. Soria-Verdugo, E. Goos, N. García-Hernando, Effect of the number of TGA curves employed on the biomass pyrolysis kinetics results obtained using the distributed activation energy model, Fuel Processing Technology 134 (2015) 360–371.
[50] B. Wang, F. Xu, P. Zong, J. Zhang, Y. Tian, Y. Qiao, Effects of heating rate on fast pyrolysis behavior and product distribution of Jerusalem artichoke stalk by using TG-FTIR and Py-GC/MS, Renew. Energy 132 (2019) 486–496.
[51] J. Komandur, R. Vinu, K. Mohanty, Pyrolysis kinetics and pyrolysate composition analysis of Mesua ferrea L: a non-edible oilseed towards the production of sustainable renewable fuel, Bioresour. Technol. 351 (2022) 126987.
[52] L.N. Samuelsson, M.U. Babler, R. Moriana, A single model-free rate expression describing both non-isothermal and isothermal pyrolysis of Norway Spruce, Fuel 161 (2015) 59–67.
[53] X. Gai, H. Wang, J. Liu, L. Zhai, S. Liu, T. Ren, H. Liu, Effects of feedstock and pyrolysis temperature on biochar adsorption of ammonium and nitrate, PLoS. One 9 (12) (2014) e113888.
[54] T. Damartzis, D. Vamvuka, S. Sfakiotakis, A. Zabaniotou, Thermal degradation studies and kinetic modeling of cardoon (Cynara cardunculus) pyrolysis using thermogravimetric analysis (TGA), Bioresour. Technol. 102 (10) (2011) 6230–6238.
[55] B. Zhao, D. O'Connor, J. Zhang, T. Peng, Z. Shen, D.C. Tsang, D. Hou, Effect of pyrolysis temperature, heating rate, and residence time on rapeseed stem derived biochar, J. Clean. Prod. 174 (2018) 977–987.
[56] A.R. Usman, A. Abduljabbar, M. Vithanage, Y.S. Ok, M. Ahmad, M. Ahmad, J. Elfaki, S.S. Abdulazeem, M.I. Al-Wabel, Biochar production from date palm waste: charring temperature induced changes in composition and surface chemistry, J. Anal. Appl. Pyrolysis. 115 (2015) 392–400.
[57] A. Lataf, M. Jozefczak, B. Vandecasteele, J. Viaene, S. Schreurs, R. Carleer, J. Yperman, W. Marchal, A. Cuypers, D. Vandamme, The effect of pyrolysis temperature and feedstock on biochar agronomic properties, J. Anal. Appl. Pyrolysis. 168 (2022) 105728.
[58] J. Zhang, J. Liu, R. Liu, Effects of pyrolysis temperature and heating time on biochar obtained from the pyrolysis of straw and lignosulfonate, Bioresour. Technol. 176 (2015) 288–291.
[59] R.K. Mishra, V. Kumar, K. Mohanty, Pyrolysis kinetics behaviour and thermal pyrolysis of Samanea saman seeds towards the production of renewable fuel, J. Energy Inst. 93 (3) (2020) 1148–1162.
[60] S. Pambudi, J.S. Jongyingcharoen, W. Saechua, Thermochemical treatment of spent coffee grounds via torrefaction: a statistical evidence of biochar properties similarity between inert and oxidative conditions, Results. Eng. 21 (2024) 102012.
[61] A. Tomczyk, Z. Sokołowska, P. Boguta, Biochar physicochemical properties: pyrolysis temperature and feedstock kind effects, Rev. Environ. Sci. Bio/Technol. 19 (1) (2020) 191–215.
[62] L. Wang, M.N.P. Olsen, C. Moni, A. Dieguez-Alonso, J.M. de la Rosa, M. Stenrød, X. Liu, L. Mao, Comparison of properties of biochar produced from different types of lignocellulosic biomass by slow pyrolysis at 600°C, Appl. Energy Combust. Sci. 12 (2022) 100090.
[63] R.K. Mishra, K. Mohanty, Bio-oil and biochar production using thermal and catalytic pyrolysis of low-value waste neem seeds over low-cost catalysts: effects of operating conditions on product yields and studies of physicochemical characteristics of bio-oil and biochar, Biochar. 3 (4) (2021) 641–656.
[64] M. Waqas, A. Aburiazaiza, R. Miandad, M. Rehan, M. Barakat, A. Nizami, Development of biochar as fuel and catalyst in energy recovery technologies, J. Clean. Prod. 188 (2018) 477–488.
[65] A. Shaaban, S.-M. Se, M. Dimin, J.M. Juoi, M.H.M. Husin, N.M.M. Mitan, Influence of heating temperature and holding time on biochars derived from rubber wood sawdust via slow pyrolysis, J. Anal. Appl. Pyrolysis. 107 (2014) 31–39.
[66] M. Waqas, A. Nizami, A. Aburiazaiza, M. Barakat, I. Ismail, M. Rashid, Optimization of food waste compost with the use of biochar, J. Environ. Manage 216 (2018) 70–81.
[67] M. Ahmad, S.S. Lee, S.E. Lee, M.I. Al-Wabel, D.C. Tsang, Y.S. Ok, Biochar-induced changes in soil properties affected immobilization/mobilization of metals/metalloids in contaminated soils, J. Soils. Sediments. 17 (2017) 717–730.
[68] Y. Ding, Y. Liu, S. Liu, Z. Li, X. Tan, X. Huang, G. Zeng, L. Zhou, B. Zheng, Biochar to improve soil fertility. A review, Agron. Sustain. Dev. 36 (2016) 1–18.
[69] G. Balmuk, M. Videgain, J.J. Manyà, G. Duman, J. Yanik, Effects of pyrolysis temperature and pressure on agronomic properties of biochar, J. Anal. Appl. Pyrolysis. 169 (2023) 105858.
[70] W.A.W.A.K. Ghani, A. Mohd, G. da Silva, R.T. Bachmann, Y.H. Taufiq-Yap, U. Rashid, H. Ala'a, Biochar production from waste rubber-wood-sawdust and its potential use in C sequestration: chemical and physical characterization, Ind. Crops. Prod. 44 (2013) 18–24.
[71] P. Giudicianni, G. Cardone, R. Ragucci, Cellulose, hemicellulose and lignin slow steam pyrolysis: thermal decomposition of biomass components mixtures, J. Anal. Appl. Pyrolysis. 100 (2013) 213–222.
[72] E.N. Yargicoglu, B.Y. Sadasivam, K.R. Reddy, K. Spokas, Physical and chemical characterization of waste wood derived biochars, Waste Manag. 36 (2015) 256–268.
[73] D.H. Itam, I.T. Horsfall, T.H. Ekiyor, Application of biochar in soil remediation: a decade of scientometrics and systematic review from 2014 to 2024, Results. Eng. 23 (2024) 102757.